NASA Technical Paper 2934

1989

Stress Corrosion Study of PH13-8Mo Stainless Steel Using the Slow Strain Rate Technique

Pablo D. Torres
George C. Marshall Space Flight Center
Marshall Space Flight Center, Alabama

NASA
National Aeronautics and Space Administration
Office of Management
Scientific and Technical Information Division

TABLE OF CONTENTS

LIST OF ILLUSTRATIONS

LIST OF TABLES

TECHNICAL PAPER

STRESS CORROSION STUDY OF PH13-8Mo STAINLESS STEEL USING THE SLOW STRAIN RATE TECHNIQUE

INTRODUCTION

A need for a rapid, reproducible, and still reliable method to characterize the susceptibility of metals to Stress Corrosion Cracking (SCC) has led many investigators to look closer at the Slow Strain Rate Technique (SSRT) during the last few decades. The purpose of the present work on PH13-8Mo stainless steel was to extend the basis for the assessment of the SSRT as a method to determine susceptibility to SCC. For that purpose, two aging conditions were evaluated on PH13-8Mo (H950 and H1000) and tests were run in neutral (air) and corrosive (3.5% NaCl) environments at several strain rates. The fracture pattern of several specimens was studied by using Scanning Electron Microscopy (SEM) analysis and the data were compared by choosing some parameters representative of changes in ductility. The ability of this method to detect differences in susceptibility to SCC of PH13-8Mo at two different aging conditions is discussed in this work. For comparison purposes, additional salt spray testing was carried out at 75 and 100 percent of the 0.2-percent offset yield strength of the material.

DESCRIPTION OF THE SLOW STRAIN RATE TECHNIQUE

The SSRT has recently emerged as a technique for studying the stress corrosion behavior of metals. It provides results in a relatively short time and shows data reproducibility. The equipment used in this technique allows for selection of the desired strain rate and test environment (Figs. 1 and 2). The test involves the application of a relatively slow strain rate to a tensile specimen under controlled-environmental conditions. Figure 3 shows a typical tensile specimen used. An aggressive environment to promote SCC and an inert environment are used, and several parameters are compared to indicate the susceptibility of the material to SCC. Several measurable and quantifiable parameters can be chosen to indicate susceptibility to SCC in Slow Strain Rate (SSR) tests by virtue of their ability to reflect loss in ductility, as the stress corrosion failures are associated with little plastic deformation during crack propagation. A load-elongation curve is obtained from each test (Fig. 4). The area under this curve (fracture energy), the elongation at fracture, the time-to-failure, and the percent of reduction-in-area (%RA) are representative of the ductility and usually indicate degree of stress corrosion susceptibility. The lower the values are in a corrosive environment, in comparison to those determined in an inert environment (all other experimental conditions being the same), the more susceptible the material is to SCC. By testing a material at different strain rates, a particular range can be obtained at which the effect of the corrosive environment on the specimen is very noticeable. Certain conditions that control the stress corrosion reaction can take place at strain rates other than the critical strain rates. Too-fast strain rates can produce tensile overload failures, while too-slow rates permit film repair on the metal. Even when the chosen parameters indicate loss in ductility at some particular strain rates, the SCC reaction has to be corroborated because hydrogen in the metal also reduces ductility and other conditions like

intergranular corrosion can also affect results. In some cases it is difficult to establish whether or not SCC events have occurred even with microstructure analysis, especially if the failures fall in the brittle-to-ductile transition region.

EXPERIMENTAL PROCEDURE

Round tensile specimens of PH13-8Mo high-strength stainless steel, 0.125 inches in diameter, 2 inches long (Fig. 3) and taken in the short transverse direction, were used in these tests. The chemical composition limits of PH13-8Mo are shown in Table 1. In order to determine the ability of the SSRT to differentiate between the resistance of PH13-8Mo to SCC at two different levels of heat treatment, the alloy was tested in the H950 and H1000 conditions. The specimens were heat treated for 4 hr at each aging temperature [510 °C (950 °F) and 538 °C (1,000 °F)] and then air cooled. All the specimens were vapor blasted to eliminate the dark oxide coat which formed on the surface as a result of the heat treatment. Several specimens were used for determination of mechanical properties, which are presented in Table 2. Prior to each test, every specimen was cleaned with denatured alcohol. A 3.5% NaCl solution was used as an aggressive solution to promote SCC and air was used as an inert test environment. Deionized water was used in the preparation of the corrosive solution. A Cortest SSR Tester was used (Fig. 1) in conjunction with an X-Y Recorder to record the amplified load signal as a function of elongation. All tests were performed at room temperature and atmospheric pressure. After threading the specimen into the machine components, the selected environment was introduced and a 100-lb (445N) load was applied to take up slack from the system. The machine was set to pull the specimen downward and the speed was controlled by adjusting the motor speed dial. The speed was displayed in revolutions per minute (rpm) which is converted to equivalent strain rate in mm/mm/sec by using a conversion factor obtained from the manufacturer's manual for the SSR Tester. Each specimen was pulled until the breaking point. At that point the system was automatically shut down and the resulting load-elongation curve and broken specimens were saved for future analysis.

Several selected broken specimens, which showed a remarkable reduction in ductility, were submitted to SEM analysis to determine the fracture pattern. A very ductile failure was also examined in order to have a basis to compare the microstructure. The loss in ductility was then expressed in terms of several parameters. The parameter values were obtained either from the produced curves or from the broken specimens. A micrometer was used to measure the final diameter in the necked-down area of the specimens to get %RA. The time-to-failure was obtained directly from a timer attached to the SSR testing machine. From each load-elongation curve, the fracture energy (area below the curve) was obtained by using a numerical method (the trapezoid rule). The elongation at fracture was also obtainable from the same curve.

Triplicate round tensile specimens of PH13-8Mo H950, stressed to 75 percent and 100 percent of the 0.2-percent offset yield strength, were also tested in salt spray as a conventional method for accelerated environmental exposure to be compared with the SSRT. The same kind of specimens as those used in SSR testing were used in salt spray. The threaded ends of the specimens were coated with Conoco HD Calcium Grease as a method of preventing crevice corrosion in the contact areas between the specimens and the fixtures. This avoids failures in regions which previous testing has shown may interfere with the SCC evaluation of this alloy. A stressing device was used to apply the desired strain followed by a surface cleaning of the samples with alcohol. The specimens were then exposed to 5 percent salt fog for 6 months.

RESULTS AND DISCUSSION

Tests were conducted on PH13-8Mo specimens in the H950 condition at strain rates between 7×10^{-7} and a 2.2×10^{-6} mm/mm/sec in a 3.5% NaCl solution and in air to get the most suitable range for testing this alloy. The load-elongation curve that was obtained after the completion of each test showed whether the test specimens failed prematurely as depicted by the curves in Figure 4. By visual examination of these curves, a tendency toward early failures was observed when testing in 3.5% NaCl at strain rates from 8.7×10^{-7} to 1.2×10^{-6} mm/mm/sec. For that reason, additional testing was done in this range attempting to reproduce this effect. The range obtained with the H950 specimens (8.7×10^{-7} to 1.2×10^{-6} mm/mm/sec) was used to test the H1000 specimens. Figures 5 and 6 show several photomicrographs of the material tested at 1.0×10^{-6} mm/mm/sec. Figure 5 shows a very ductile failure from a test run in air. Figure 6 shows a more brittle fracture, which is consistent with an early failure of the sample caused by the 3.5 percent salt solution. Even though no clear evidence of stress corrosion was seen, the reduction in ductility appears to be related to susceptibility to SCC.

The following parameters were chosen to express loss in ductility: %RA, time-to-failure, elongation at fracture, and fracture energy. The data obtained from these parameters are presented in Tables 3 to 6. Other parameters, for example maximum load and fracture load, were found not to be appropriate for measuring loss in ductility when testing this particular alloy. To keep a constant approach and because most of the time the variation of the values in air was slight compared to the variation in 3.5% NaCl, the ratio of each parameter in 3.5% NaCl to the average of the same parameter in air was calculated for each strain rate and aging condition and the results are presented in Table 7. The loss in ductility previously observed in the load-elongation curves was then translated in terms of those ratios to measure the degree of susceptibility to SCC. Those ratios were plotted against the strain rate and are presented in Figures 7 to 14. Eight out of the 20 (40 percent) specimens in the H950 condition tested in 3.5% NaCl showed reduction in ductility when tests were conducted at $1 \pm 0.2 \times 10^{-6}$ mm/mm/sec. No reduction in ductility occurred in air. This delineates a minimum in either one of the parameter ratios versus strain rate curves in the H950 specimens, as seen from Figures 7 to 10. All four parameters appeared to show sensitivity to ductility changes. The need to conduct several tests at the same conditions, in order to get the critical strain rate, is apparent as seen from the variation of the data points in Figures 7 to 10.

The specimens in the H1000 condition, tested in 3.5 percent salt at the critical strain rate, showed much less tendency to loose ductility than the H950 specimens, as seen from Figures 11 to 14. This shows that even though PH13-8Mo is not immune to SCC in the H1000 condition, it is more resistant than it is in the H950 condition. No failures occurred in the salt spray test conducted during this program (Table 8), however, previous MSFC data [1], as well as an Armco 18-year test at the seacoast [2] show that the resistance of PH13-8Mo to SCC increases with aging temperature, which is consistent with the slow strain rate results. This shows that the SSRT could give quick indications of the results that could be expected using conventional methods.

CONCLUSIONS

The results of this investigation show that the SSRT is capable of establishing a difference in SCC susceptibility between PH13-8Mo H950 and PH13-8Mo H1000 when testing this alloy in 3.5 percent salt

water and air, based on ductility changes. This suggests that PH13-8Mo should be heat treated at 538 °C (1,000 °F) or preferably higher if good SCC resistance is desired, as long as the attained mechanical properties remain acceptable for the particular application. In addition, a shorter test period is required by using this technique than when using conventional methods.

The critical strain rate to promote reduction in ductility (which has been used to measure susceptibility to SCC) in a 3.5% NaCl solution was found to be in the vicinity of 1.0×10^{-6} mm/mm/sec for this alloy. %RA, time-to-failure, elongation at fracture, and fracture energy were found to be adequate parameters for expressing the degree of susceptibility to SCC. Several specimens need to be tested at the same conditions, as the tested material can behave differently at the same strain rate.

Previous studies on PH stainless steel [1,2] favor salt spray and seacoast for the stress corrosion evaluation of this alloy, and its results agree with those obtained with the SSRT. Even though this technique was shown to provide a quick indication of what could be expected in a more time-consuming conventional test, certain precautions should be taken because results obtained by this method do not necessarily always correspond to those from conventional techniques when testing other materials. The SSRT has shown to be promising in SCC evaluation of metal alloys, and more research is encouraged to fully assess the validity of this technique and its applicability in the screening of metallic materials for stress corrosion resistance.

REFERENCES

1. Humphries, T.S. and Nelson, E.E.: Stress Corrosion Cracking Evaluation of Martensitic Precipitation Hardening Stainless Steels. NASA TM-78257, January, 1980.

2. Gaugh, R.R.: Stress Corrosion Cracking of Precipitation – Hardening Stainless Steels, Materials Performance. NACE, Vol. 26, No. 2, February 1987, pp. 29-34.

3. Armco Advanced Materials, Technical Data Manual, S33d (PH13-8Mo), Armco Steel Corporation.

4. Humphries, T.S. and Nelson, E.E.: Stress Corrosion Cracking Evaluation of Several Precipitation Hardening Stainless Steels. NASA TM-53910, September 12, 1969.

5. Buhl, H.: Validity of the Slow Straining Test Method in the Stress Corrosion Cracking Research Compared With Conventional Testing Techniques, Stress Corrosion Cracking – The Slow Strain Rate Technique. ASTM STP 665, G. M. Ugiansky and J. H. Payer, Eds., ASTM, 1979, pp. 336-337.

6. Payer, J.H., Berry, W.E., and Boyd, W.K.: Evaluation of Slow Strain-Rate Stress Corrosion Test Results, Stress Corrosion Cracking – The Slow Strain Rate Technique. ASTM STP 665, G. M. Ugiansky and J. H. Payer, Eds., ASTM, 1979, pp. 61-77.

7. Parkins, R.N.: Development of Strain-Rate Testing and Its Implications, Stress Corrosion Cracking – The Slow Strain Rate Technique. ASTM STP 665, G. M. Ugiansky and J. H. Payer, Eds., ASTM, 1979, pp. 5-9.

TABLE 1. COMPOSITION OF PH13-8Mo

(According to Reference 2)

	%		%
Carbon	.05 max	Chromium	12.25-13.25
Manganese	.10 max	Nickel	7.5-8.5
Phosphorous	.010 max	Aluminum	.9-1.35
Sulfur	.008 max	Molybdenum	2.00-2.50
Silicon	.10 max	Nitrogen	.01 max

TABLE 2. MECHANICAL PROPERTIES OF PH13-8Mo IN THE H950* AND H1000** CONDITIONS

	0.2% YS		UTS		%EL	%RA
	MPa	KSI	MPa	KSI		
PH13-8Mo H950	1420	206	1558	226	13.0	49.7
PH13-8Mo H1000	1358	197	1455	211	13.7	51.6

* Heat treated 4 hours at 950°F (510°C), air cool.

** Heat treated 4 hours at 1000°F (538°C), air cool.

Average of 6 specimens

TABLE 3. PERCENT OF REDUCTION IN CROSS SECTIONAL AREA DATA

Strain Rate (mm/mm/sec x10^7	%RA PH13-8Mo H950 3.5% NaCl	PH13-8Mo H950 Air	PH13-8Mo H1000 3.5%NaCl	PH13-8Mo H1000 Air
7.2	47.0	19.7		
8.7	7.8	49.3	51.6	50.4
	44.6	50.4	58.0	57.0
	48.2	39.8	57.0	53.8
		AVG=46.5		AVG=53.7
9.4	4.7	47.0	51.6	51.6
	7.8	48.2	50.4	57.0
	54.8	47.0	52.7	49.3
	18.3	AVG=47.4	57.0	AVG=52.6
	52.7		54.8	
10.1	4.7	43.4	49.3	43.4
	3.2	47.0	7.8	57.0
	47.0	48.2	53.8	57.0
	51.6	AVG=46.2	52.7	AVG=52.5
	50.4			
10.8	52.7	47.0	55.9	54.8
	42.2	52.7	54.8	52.7
	6.3	49.3	58.0	53.8
	9.4	AVG=49.7	57.0	AVG=53.5
11.6	36.0	50.4	55.9	48.2
	49.3	50.4	58.0	55.9
	49.3	52.7	57.0	54.8
		AVG=51.2		AVG=53.0
12.3	45.8	39.8		
13.0	50.4	33.4		
		44.6		
		AVG=39.0		
13.8	18.3	24.0		
15.9	48.2	52.7		
18.8	43.4	45.8		
21.7	43.4	28.1		

TABLE 4. TIME-TO-FAILURE DATA

Strain Rate (mm/mm/sec x10^7)	Time-to-Failure (hr.) PH13-8Mo H950 3.5% NaCl	PH13-8Mo H950 Air	PH13-8Mo H1000 3.5%NaCl	PH13-8Mo H1000 Air
7.2	22.4	17.5		
8.7	16.7	16.9	18.7	18.8
	20.1	22.4	22.2	22.1
	20.8	20.5	21.9	20.6
		AVG=19.9		AVG=20.5
9.4	8.5	18.2	18.6	18.1
	14.9	20.6	18.1	19.8
	22.6	18.7	19.1	19.2
	15.1	AVG=19.2	20.7	AVG=19.0
	19.8		21.6	
10.1	9.7	16.8	14.2	14.9
	8.0	17.9	11.4	19.0
	18.2	17.9	19.3	18.7
	19.2	AVG=17.5	19.4	AVG=17.6
	19.1			
10.8	16.7	15.4	15.2	14.1
	16.4	17.5	17.5	16.8
	9.0	17.2	18.7	16.9
	12.5	AVG=16.7	17.8	AVG=15.9
11.6	13.9	14.8	14.4	13.7
	16.4	16.9	16.4	17.2
	16.4	16.5	16.1	16.4
		AVG=16.1		AVG=15.8
12.3	13.5	13.6		
13.0	12.5	10.5		
		13.5		
		AVG=11.8		
13.8	11.1	8.9		
15.9	10.8	10.0		
18.8	9.0	8.3		
21.7	7.8	6.3		

TABLE 5. ELONGATION AT FRACTURE DATA

Strain Rate (mm/mm/sec x10^7)	PH13-8Mo H950 3.5% NaCl mm	inches	Air mm	inches	PH13-8Mo H1000 3.5% NaCl mm	inches	Air mm	inches
7.2	1.35	.053	.64	.025				
8.7	1.12	.044	1.42	.056	1.12	.044	1.37	.054
	1.57	.062	1.88	.074	2.11	.083	2.01	.079
	1.70	.067	1.68	.066	2.21	.087	1.73	.068
			AVG=1.66	AVG=.065			AVG=1.70	AVG=.067
9.4	0.20	.008	1.37	.054	1.73	.068	1.40	.055
	0.56	.022	2.34	.092	1.93	.076	1.83	.072
	3.12	.123	1.93	.076	1.57	.062	1.93	.076
	1.07	.042	AVG=1.88	AVG=.074	1.96	.077	AVG=1.72	AVG=.068
	1.65	.065			2.64	.104		
10.1	0.58	.023	1.35	.053	0.91	.036	1.12	.044
	0.38	.015	2.01	.079	0.64	.025	2.24	.088
	1.83	.072	1.65	.065	2.03	.080	1.73	.068
	1.93	.076	AVG=1.67	AVG=.066	1.88	.074	AVG=1.70	AVG=.067
	1.73	.068						
10.8	1.63	.064	1.35	.053	1.40	.055	1.12	.044
	1.93	.076	1.93	.076	1.75	.069	1.70	.067
	0.36	.014	2.13	.084	2.24	.088	2.34	.092
	0.74	.029	AVG=1.80	AVG=.071	2.08	.082	AVG=1.72	AVG=.068
11.6	0.97	.038	1.88	.074	1.78	.070	1.57	.062
	1.73	.068	1.93	.076	2.24	.088	2.03	.080
	1.93	.076	1.98	.078	1.96	.077	2.24	.088
			AVG=1.93	AVG=.076			AVG=1.95	AVG=.077
12.3	1.12	.044	1.88	.074				
13.0	1.09	.043	0.81	.032				
			1.85	.073				
			AVG=1.33	AVG=.052				
13.8	0.91	.036	0.81	.032				
15.9	1.57	.062	1.57	.062				
18.8	1.30	.051	1.42	.056				
21.7	1.52	.060	0.81	.032				

TABLE 6. FRACTURE ENERGY DATA

Strain Rate (mm/mm/sec X10^7)	Fracture Energy PH13-8Mo H950 3.5% NaCl N-M	3.5% NaCl in-Lb	Air N-M	Air in-Lb	PH13-8Mo H1000 3.5% NaCl N-M	3.5% NaCl in-Lb	Air N-M	Air in-Lb
7.2	13.1	116	6.2	55				
8.7	11.4	101	13.2	117	10.4	92	13.0	115
	16.0	142	19.3	171	19.4	172	19.0	168
	17.5	155	17.3	153	20.2	179	16.0	142
			AVG=16.6	AVG=147			AVG=16.0	AVG=142
9.4	1.5	13	13.7	121	16.4	145	12.8	113
	6.2	55	24.2	214	17.9	158	17.1	151
	30.8	273	19.0	168	15.0	133	18.5	164
	10.6	94	AVG=19.0	AVG=168	18.8	166	AVG=16.2	AVG=143
	16.8	149			24.9	220		
10.1	4.6	41	13.8	122	8.4	74	10.4	92
	2.5	22	20.3	180	5.4	48	20.8	184
	18.6	165	17.1	151	19.4	172	16.0	142
	19.7	174	AVG=17.1	AVG=151	17.9	158	AVG=15.7	AVG=139
	18.0	159						
10.8	16.4	145	13.6	120	12.8	113	10.5	93
	19.5	173	20.0	177	16.5	146	15.8	140
	3.1	27	21.0	186	20.7	183	21.4	189
	7.7	68	AVG=18.2	AVG=161	19.5	173	AVG=15.9	AVG=141
11.6	10.1	89	18.0	159	15.9	141	14.4	127
	17.4	154	19.4	172	20.6	182	19.7	174
	19.4	172	20.0	177	18.3	162	21.0	186
			AVG=19.1	AVG=169			AVG=18.3	AVG=162
12.3	11.3	100	18.3	162				
13.0	11.1	98	8.0	71				
			18.3	162				
			AVG=13.1	AVG=116				
13.8	9.5	84	7.5	66				
15.9	15.9	141	15.3	135				
18.8	13.4	119	14.0	124				
21.7	15.6	138	8.0	71				

TABLE 7. PARAMETER RATIOS

(Value in 3.5% NaCl/Value in Air)

Strain Rate (mm/mm/sec X10^7)	PH13-8Mo H950				PH13-8Mo H1000			
	%RA	Time	Elong	FE*	%RA	Time	Elong	FE*
7.2	2.39	1.28	2.12	2.10				
8.7	.17	.84	.68	.69	.96	.91	.66	.65
	.96	1.01	.95	.97	1.08	1.08	1.24	1.21
	1.04	1.05	1.03	1.05	1.06	1.07	1.30	1.26
9.4	.10	.44	.11	.08	.98	.98	1.00	1.01
	.16	.78	.30	.33	.96	.95	1.12	1.10
	1.16	1.18	1.66	1.62	1.00	1.01	.91	.93
	.39	.79	.57	.56	1.08	1.09	1.13	1.16
	1.11	1.03	.88	.89	1.04	1.14	1.53	1.54
10.1	.10	.55	.35	.27	.94	.81	.54	.53
	.07	.46	.23	.15	.15	.65	.37	.35
	1.02	1.04	1.09	1.09	1.02	1.10	1.19	1.24
	1.12	1.10	1.15	1.15	1.00	1.10	1.10	1.14
	1.09	1.09	1.03	1.05				
10.8	1.06	1.00	.90	.90	1.04	.96	.81	.80
	.85	.98	1.07	1.07	1.02	1.10	1.01	1.04
	.13	.54	.20	.17	1.08	1.18	1.29	1.30
	.19	.75	.41	.42	1.07	1.12	1.21	1.23
11.6	.70	.86	.50	.53	1.05	.91	.91	.87
	.96	1.02	.89	.91	1.09	1.04	1.14	1.12
	.96	1.02	1.00	1.02	1.08	1.02	1.00	1.00
12.3	1.15	.99	.59	.62				
13.0	1.29	1.06	.83	.84				
13.8	.76	1.25	1.12	1.27				
15.9	.91	1.08	1.00	1.04				
18.8	.95	1.08	.91	.96				
21.7	1.54	1.24	1.88	1.94				

*FE Denotes Fracture Energy

TABLE 8. SALT SPRAY TEST RESULTS OF PH13-8Mo H950

Stress Direction	Percent of Y.S.	Applied Stress MPa	Applied Stress KSI	5% Salt Spray Failure Ratio	5% Salt Spray Days to Failure
Short Trans.	75	1060	154	0/3	--
Short Trans.	100	1420	206	0/3	--

UTS = 1560 MPa (226 KSI)

YS = 1420 MPa (206 KSI)

Total Exposure Time was 6 Months

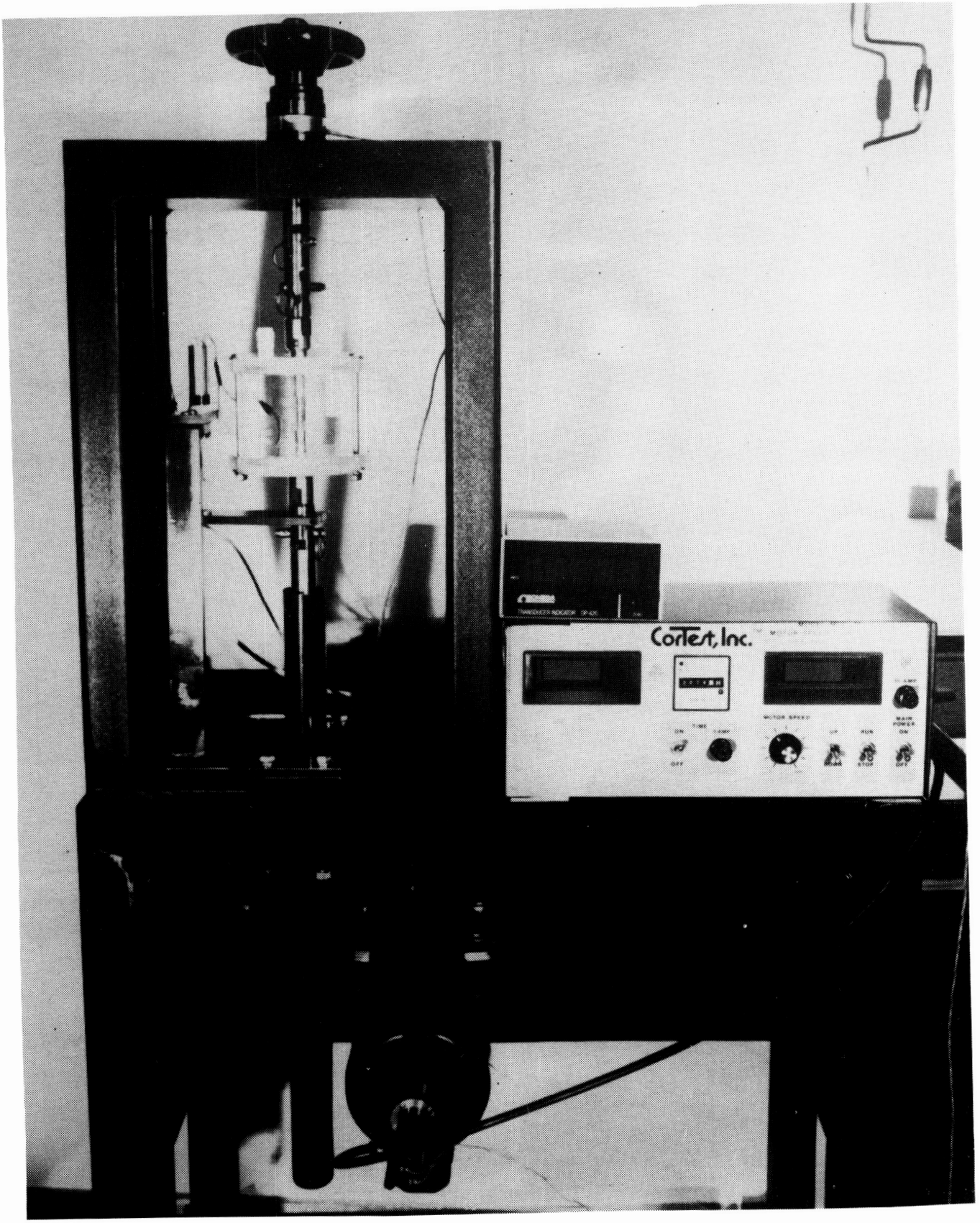

Figure 1. Slow strain rate testing machine.

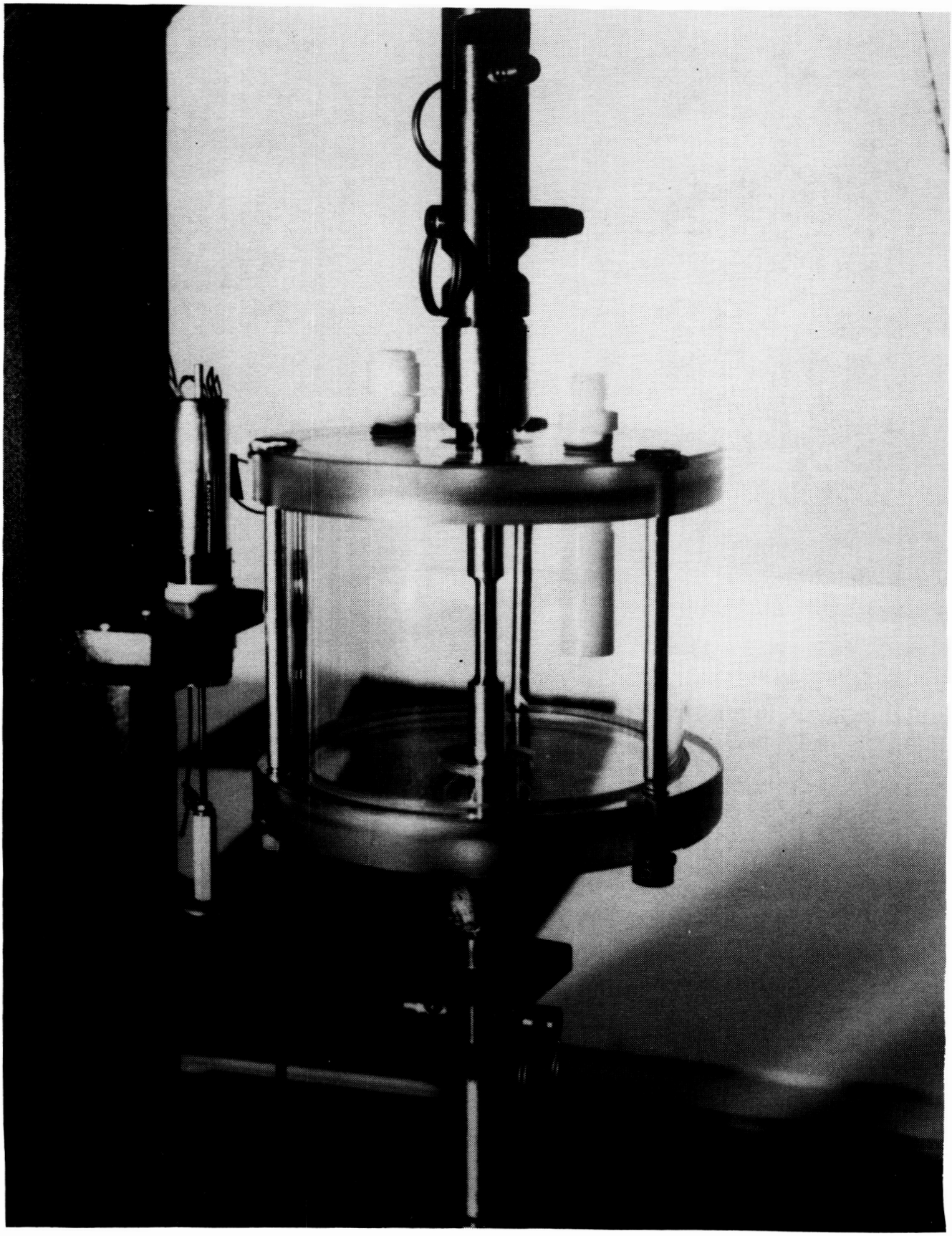

Figure 2. Feature for environment selection.

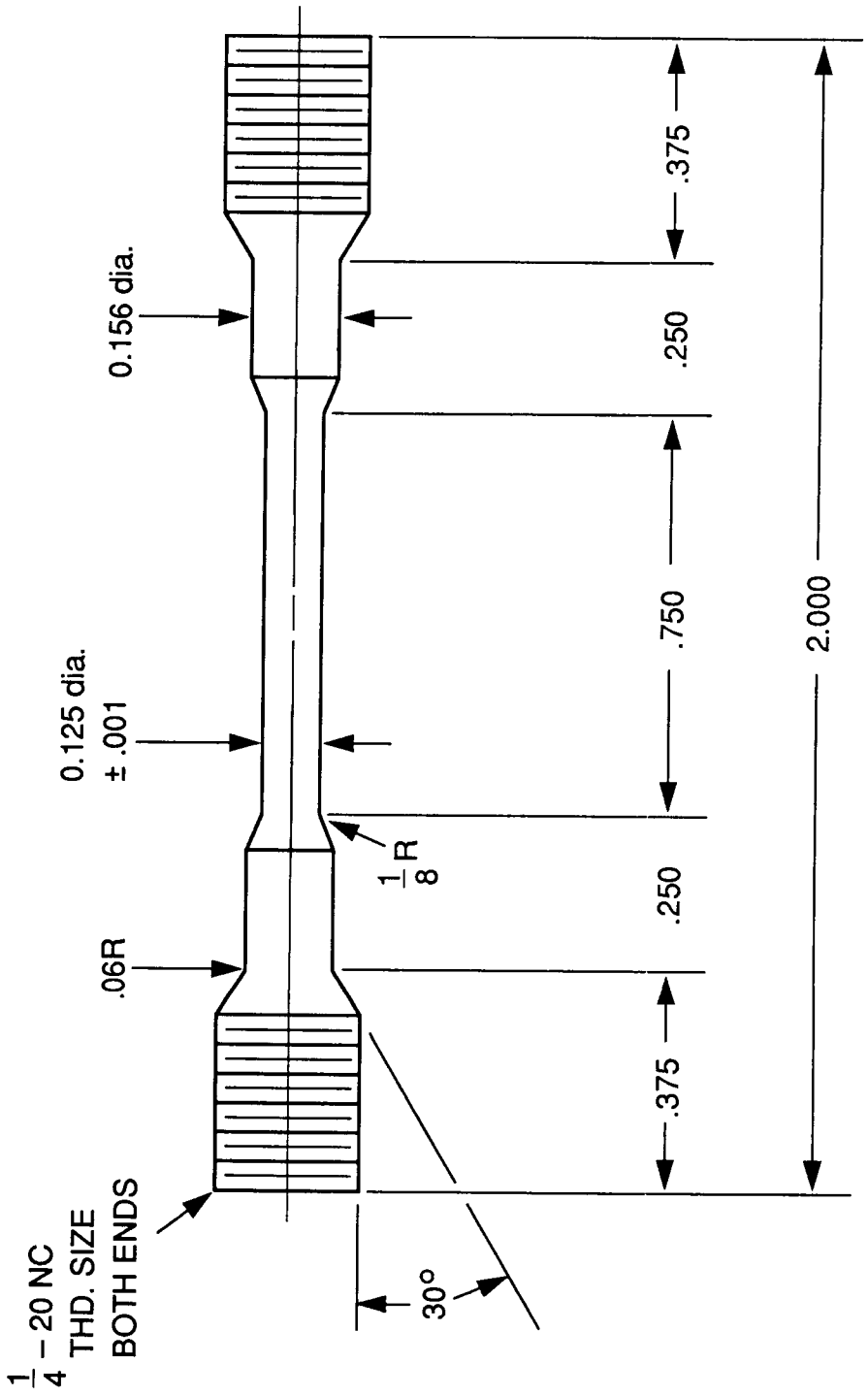

Figure 3. Round tensile specimen.

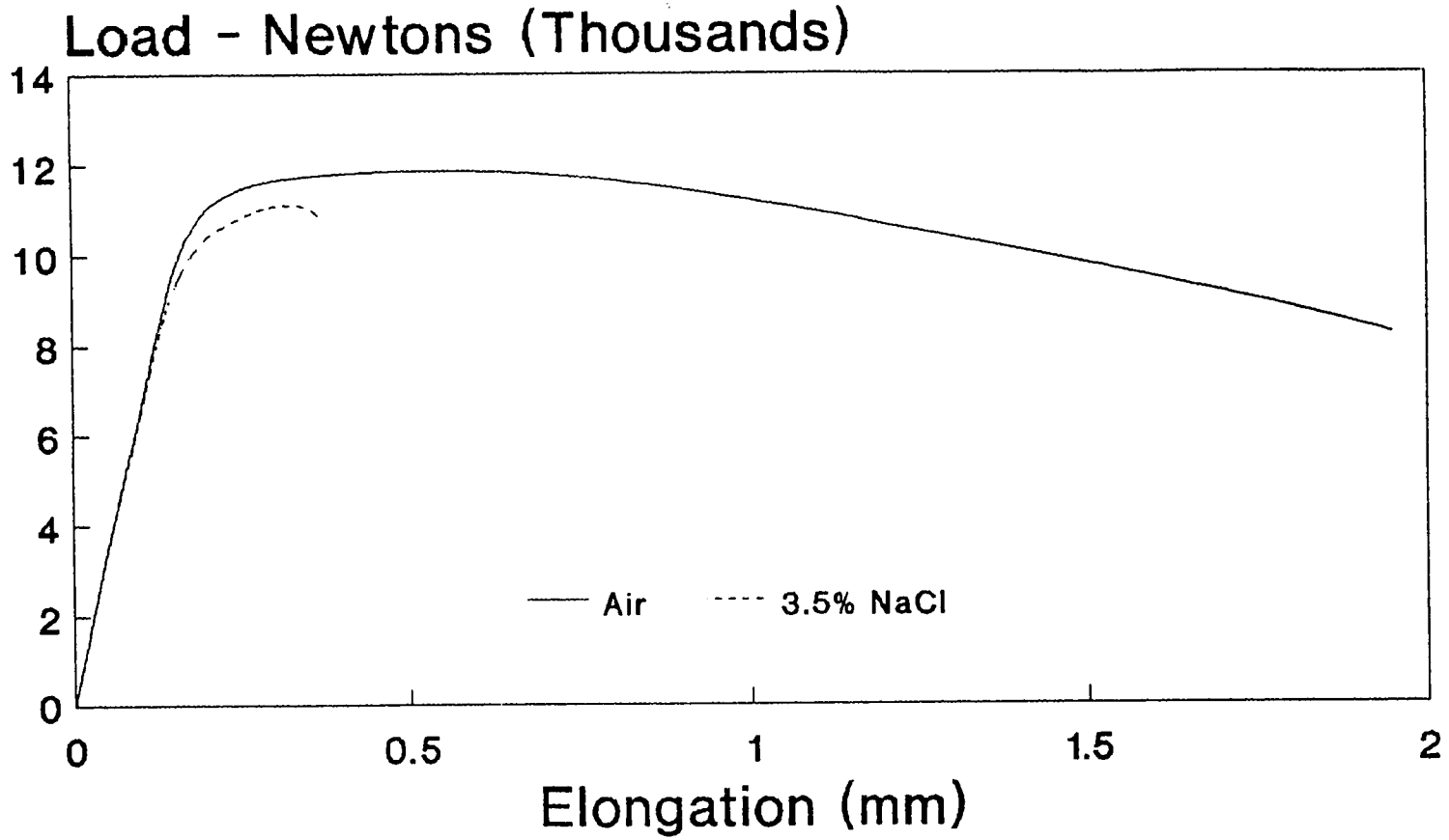

Figure 4. Load versus elongation – PH13-8Mo H950.
(Strain rate = 1×10^{-6} mm/mm/sec).

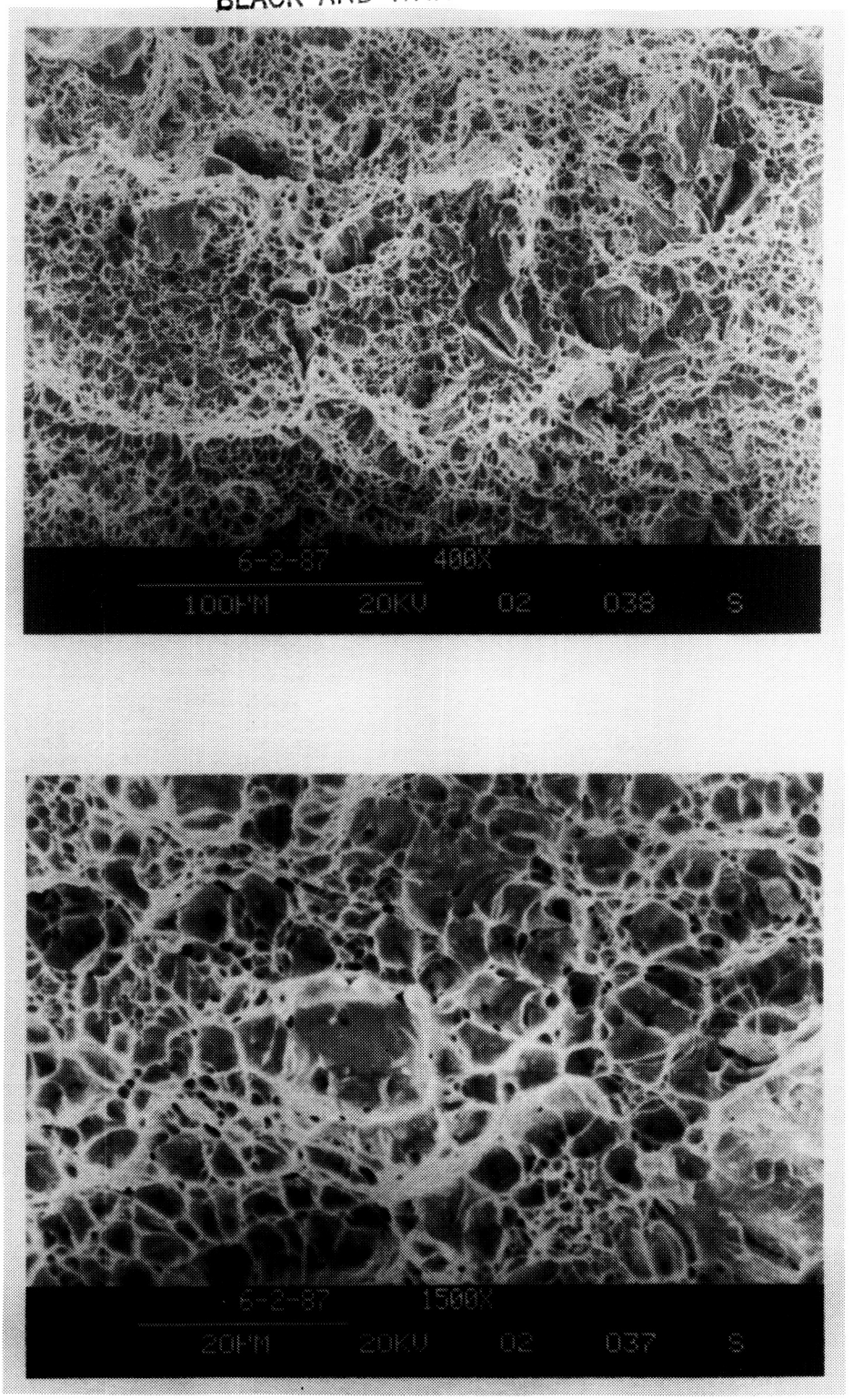

Figure 5. Photomicrographs of a PH13-8Mo H1000 SSR failed specimen tested at 1.0×10^{-6} mm/mm/sec in air.

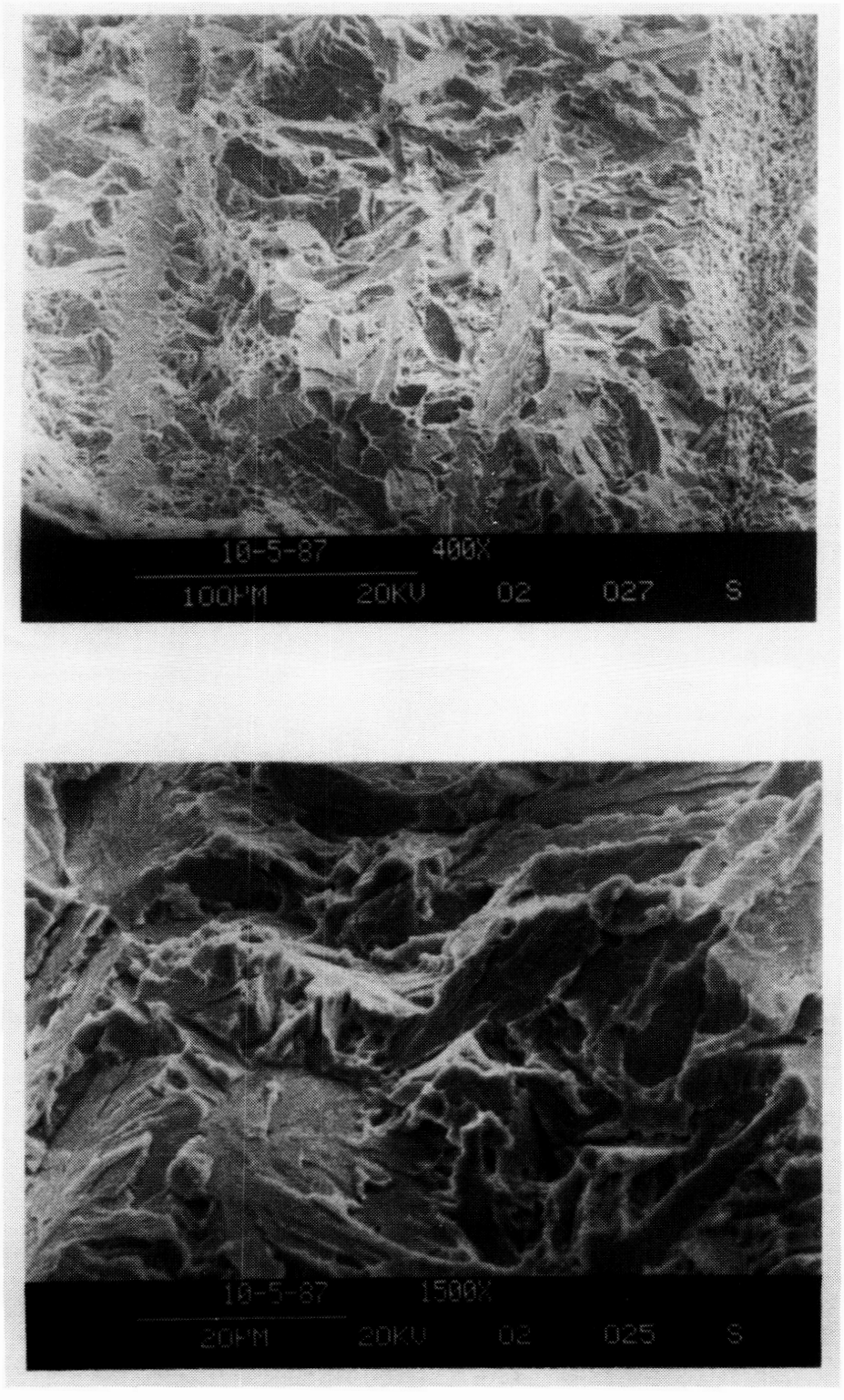

Figure 6. Photomicrographs of a PH13-8Mo H950 SSR failed specimen tested at 1.0×10^{-6} mm/mm/sec in 3.5% NaCl.

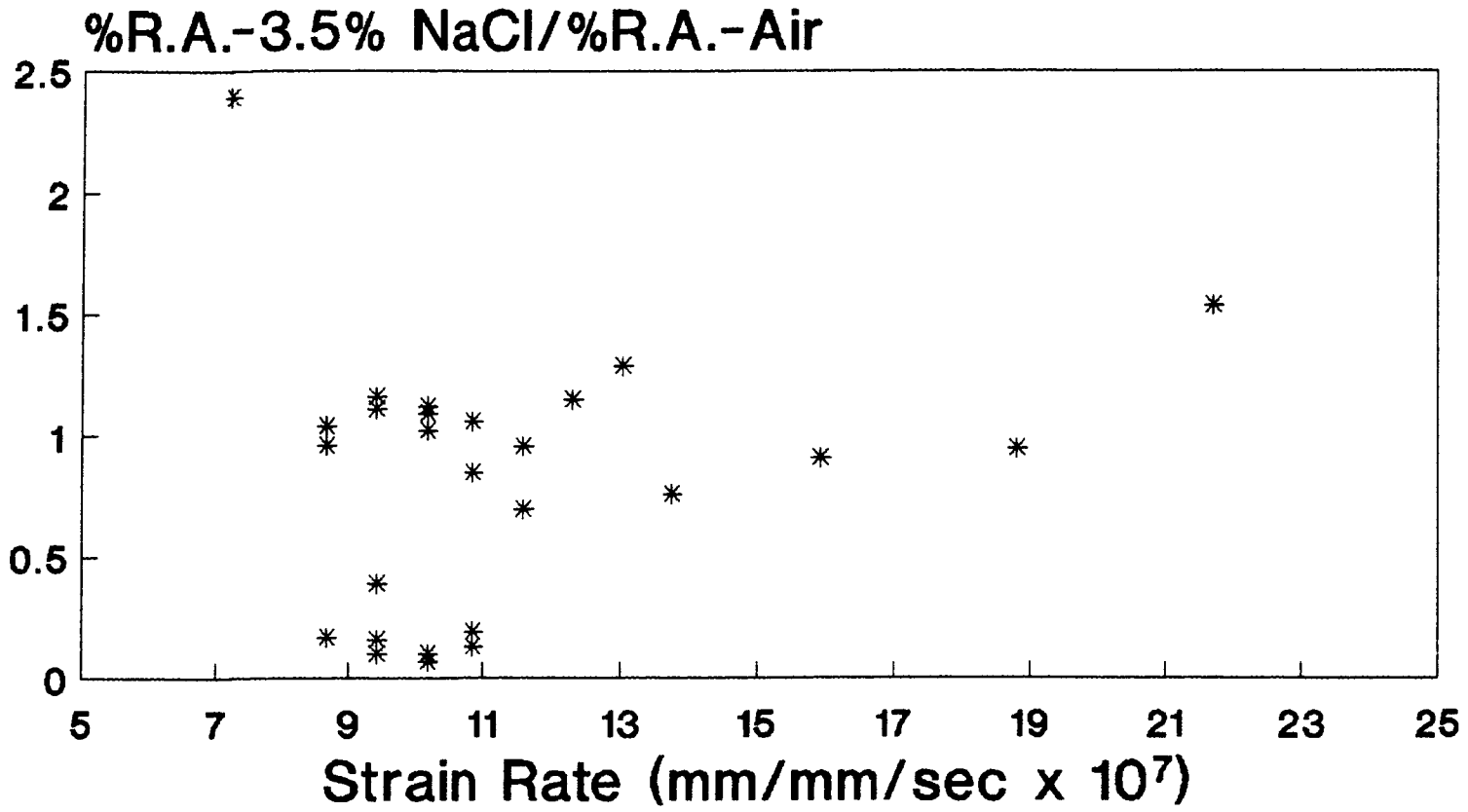

Figure 7. Reduction-in-area ratio versus strain rate PH13-8Mo H950.

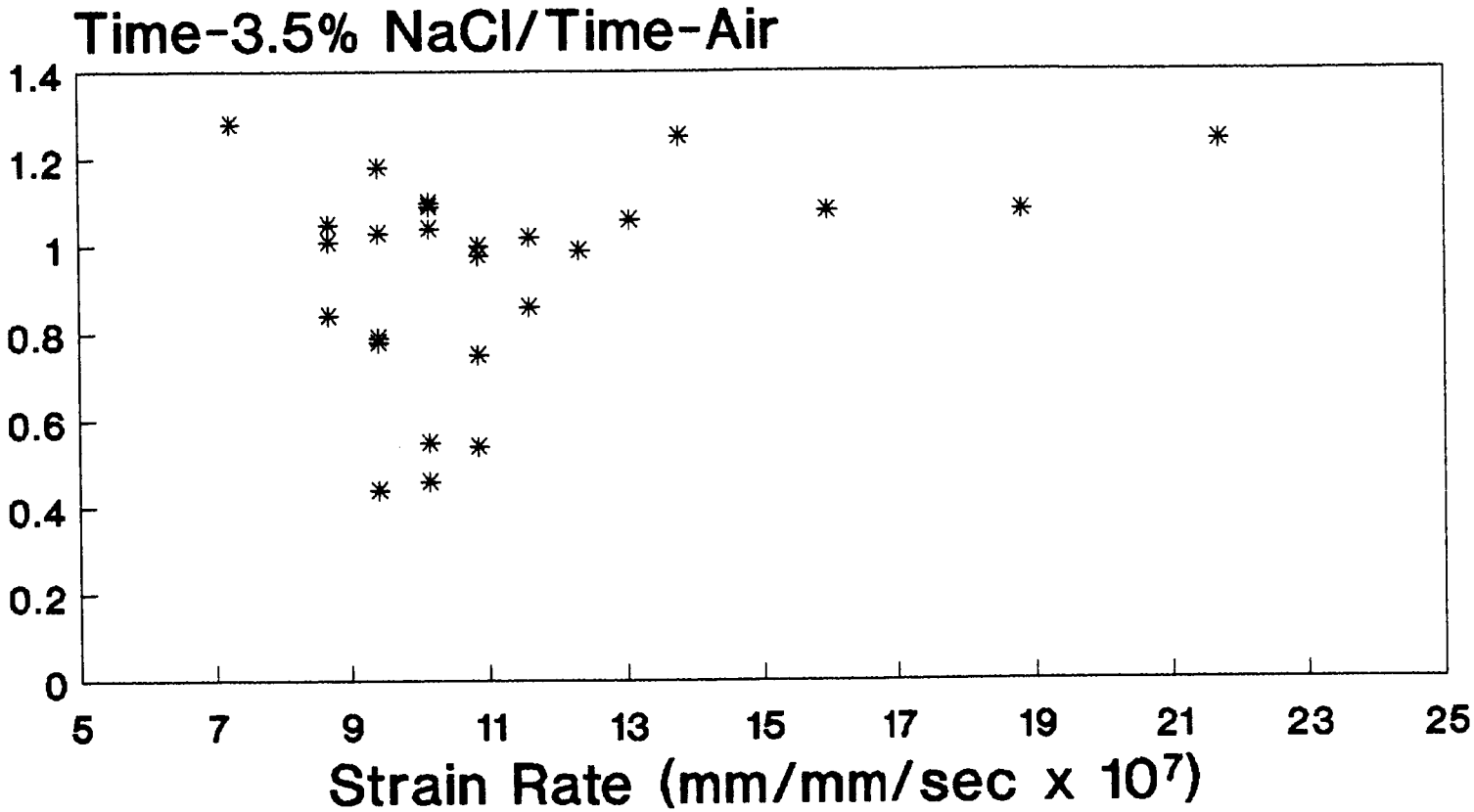

Figure 8. Time-to-failure ratio versus strain rate PH13-8Mo H950.

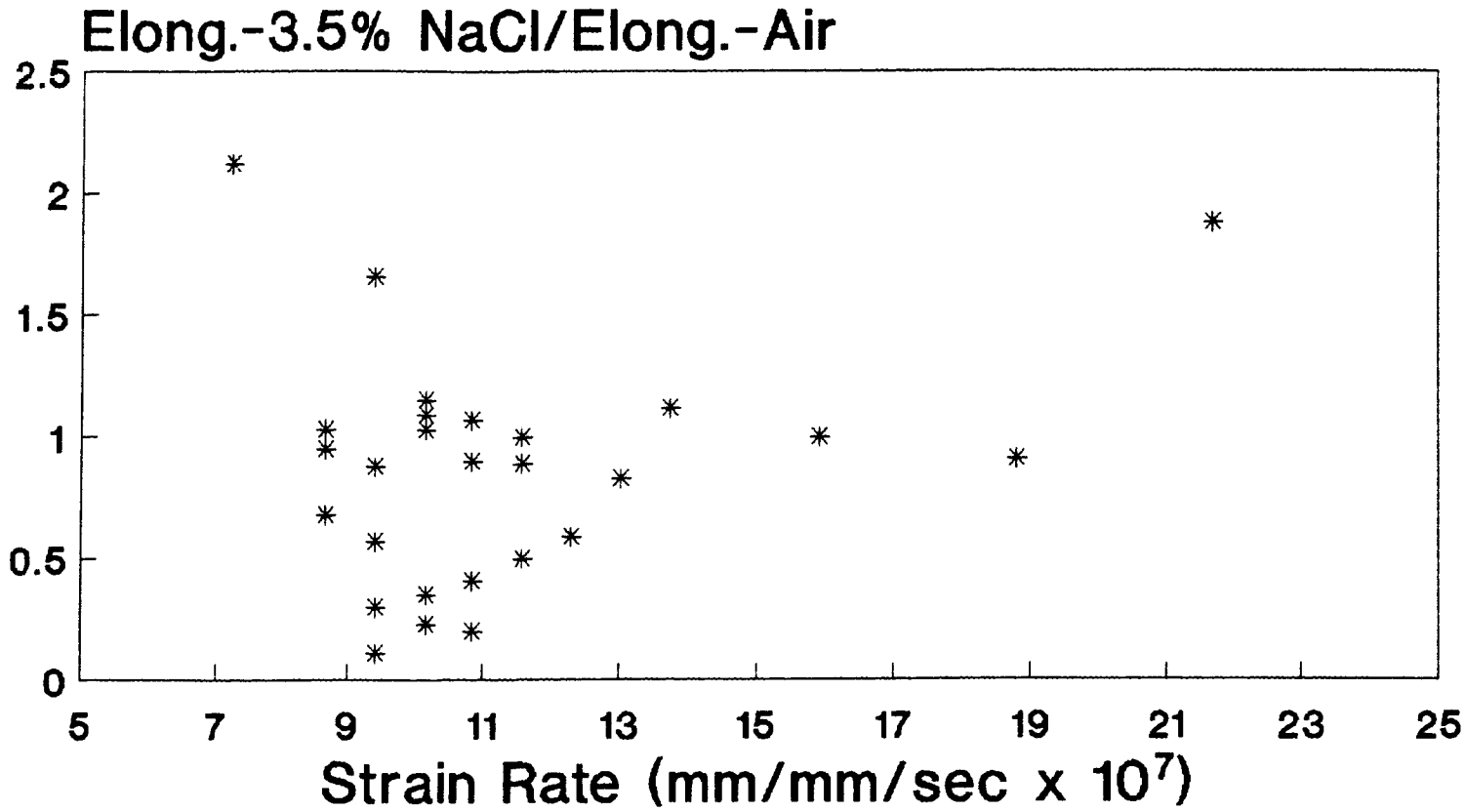

Figure 9. Elongation ratio versus strain rate PH13-8Mo H950.

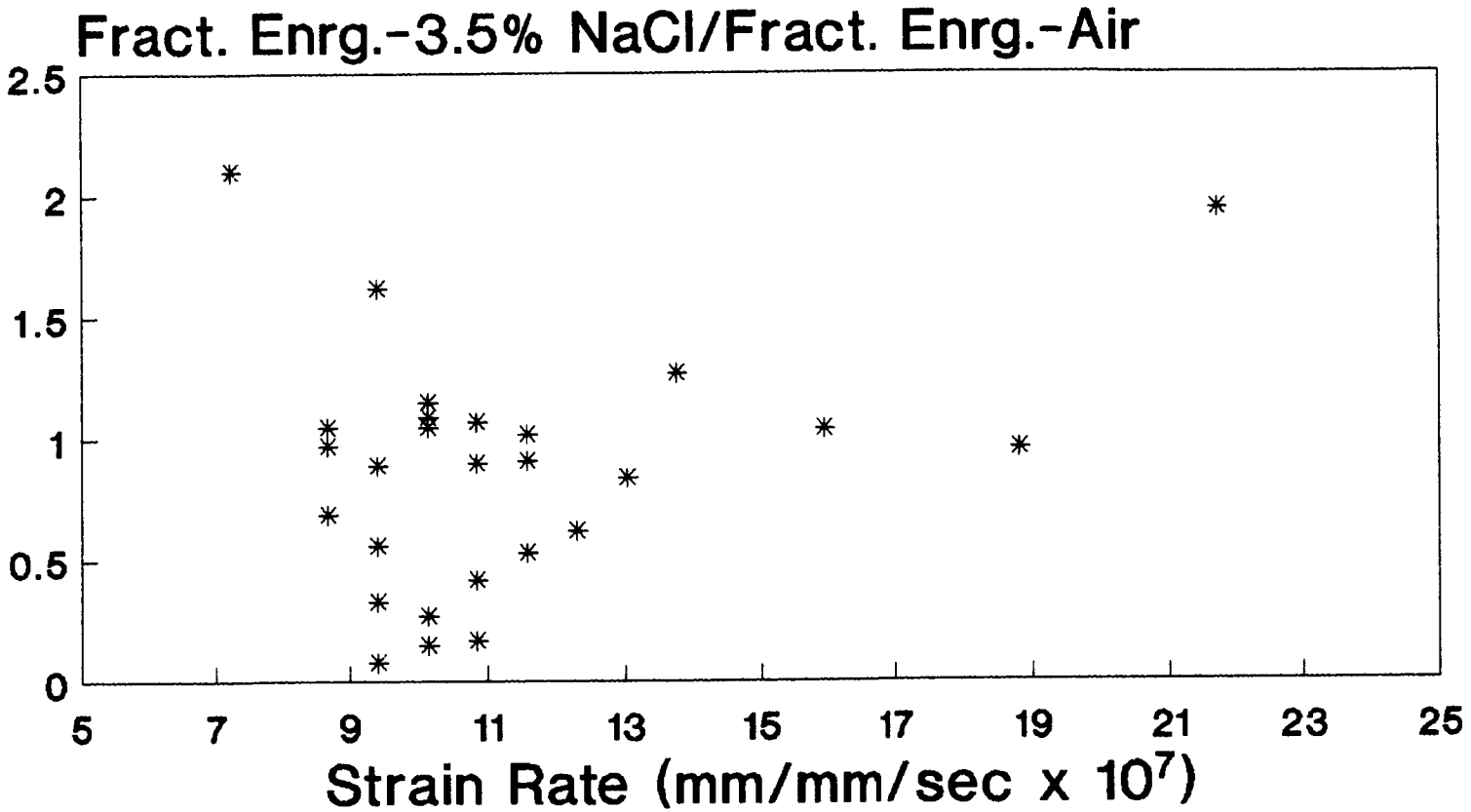

Figure 10. Fracture energy ratio versus strain rate PH13-8Mo H950.

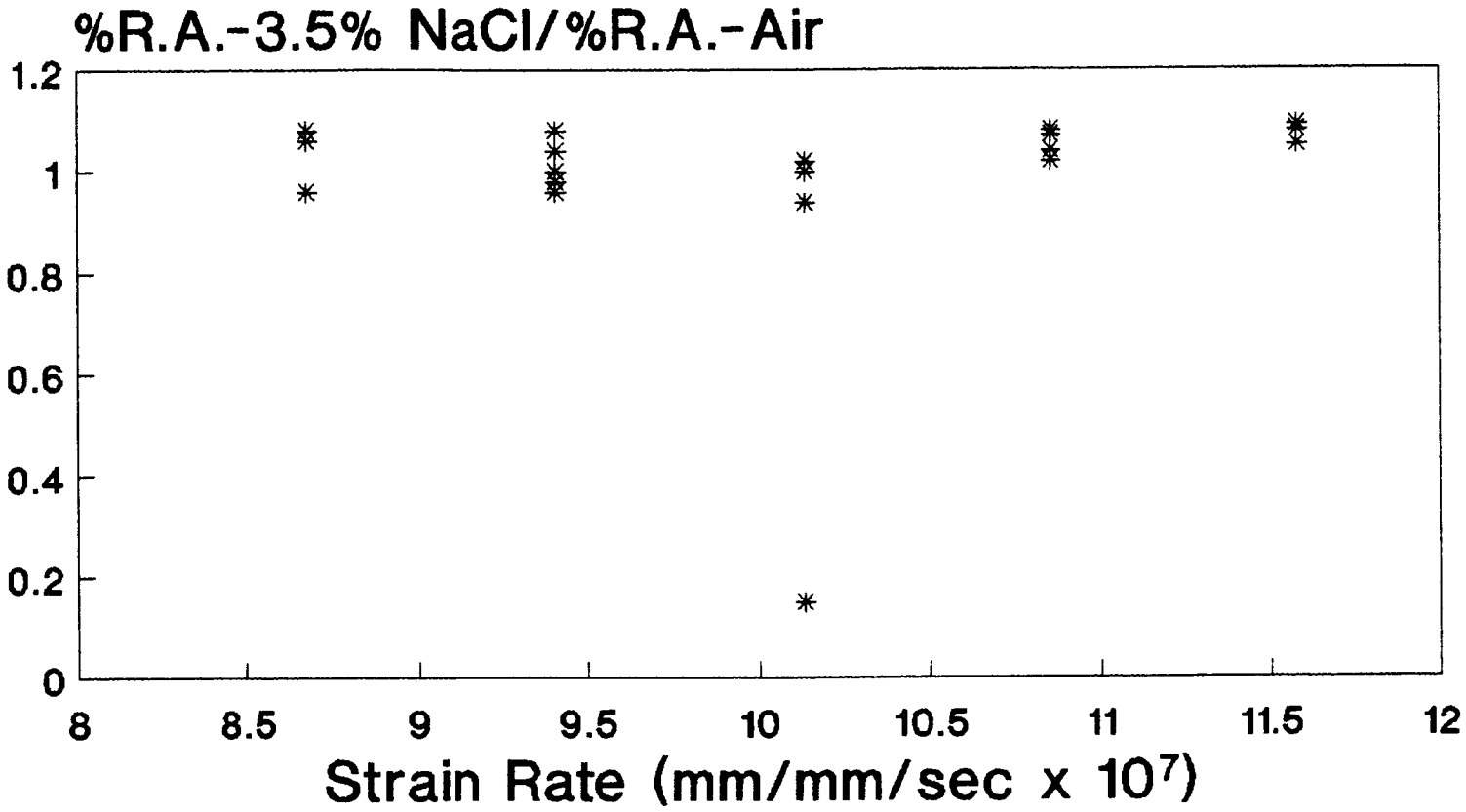

Figure 11. Reduction-in-area ratio versus strain rate PH13-8Mo H1000.

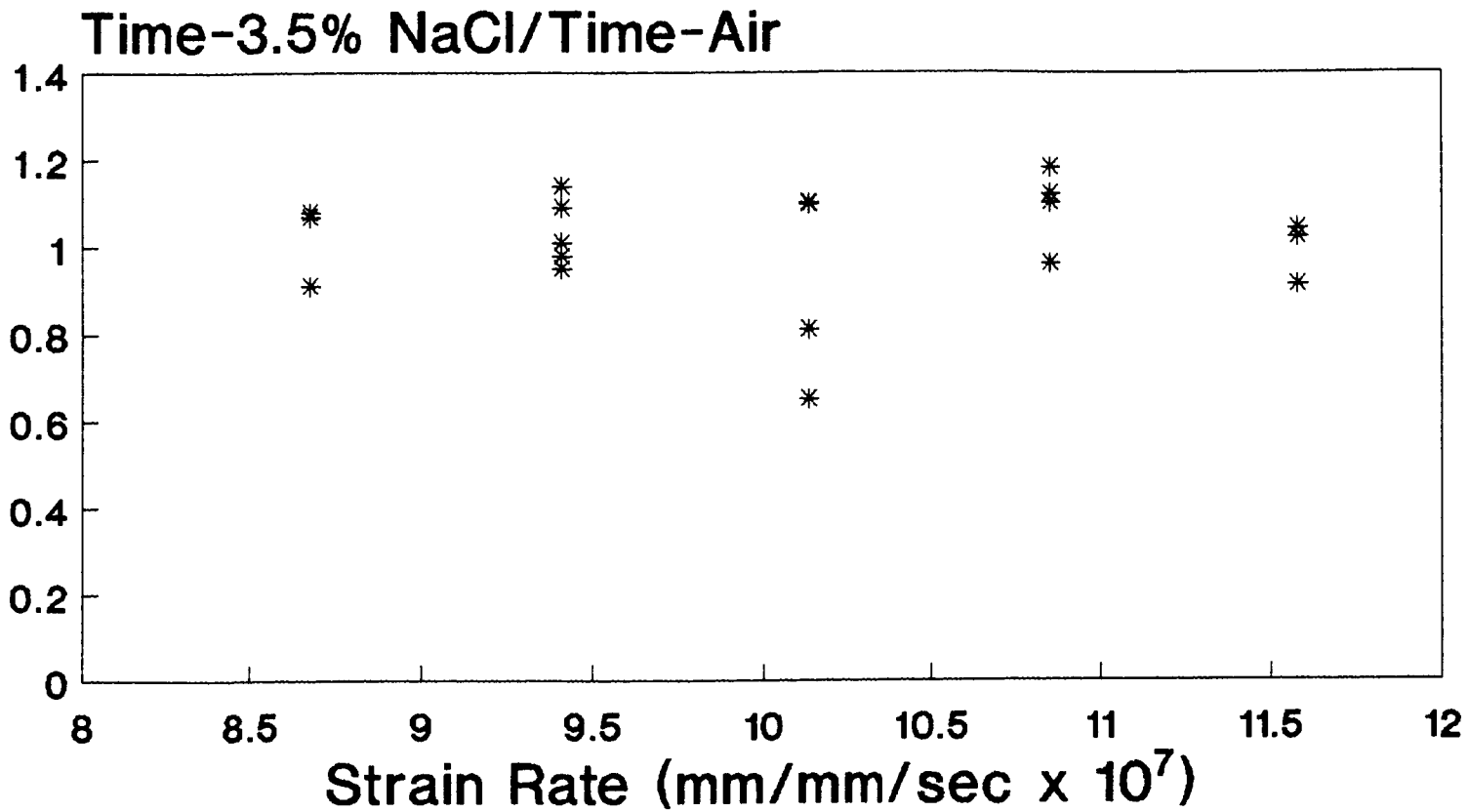

Figure 12. Time-to-failure ratio versus strain rate PH13-8Mo H1000.

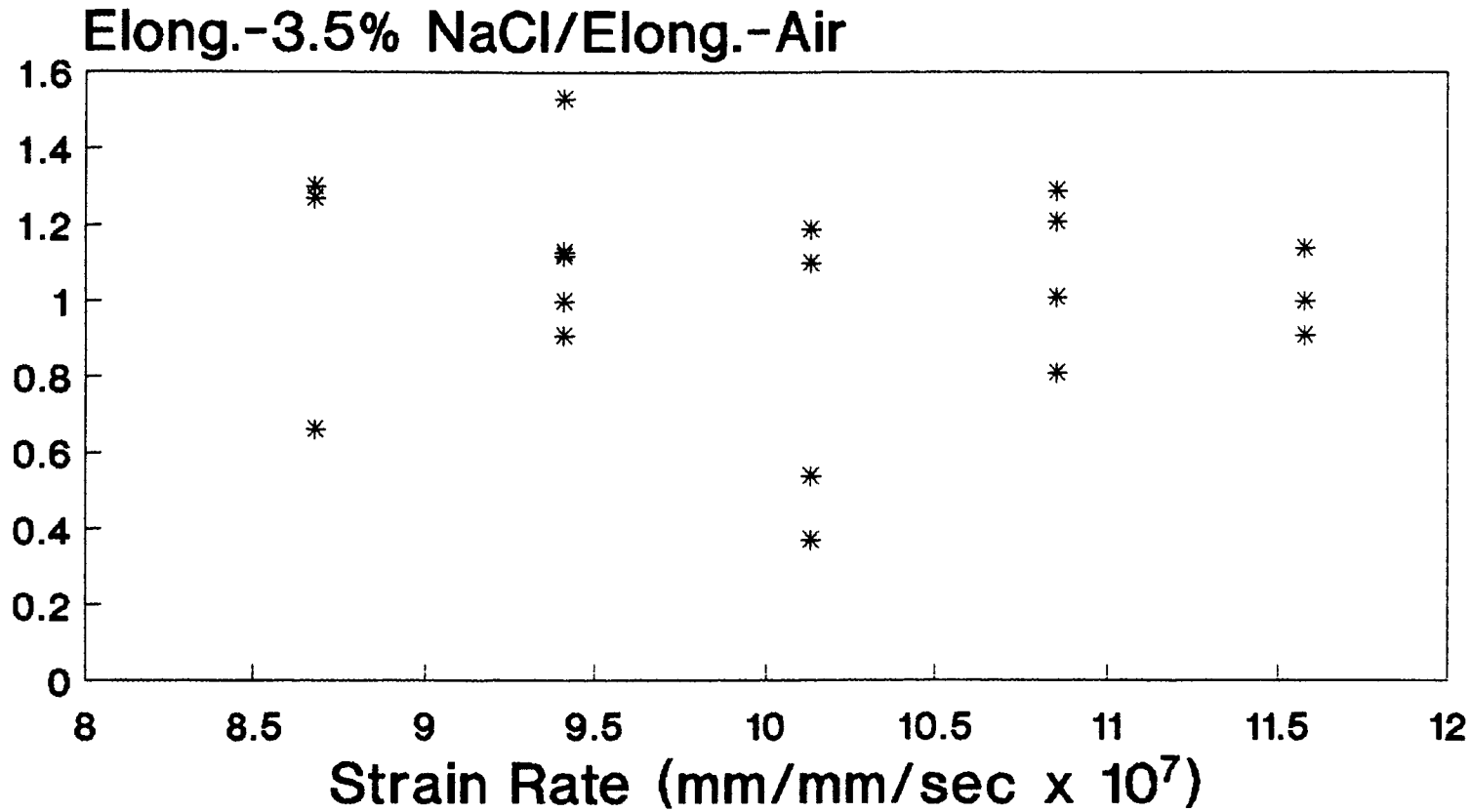

Figure 13. Elongation ratio versus strain rate PH13-8Mo H1000.

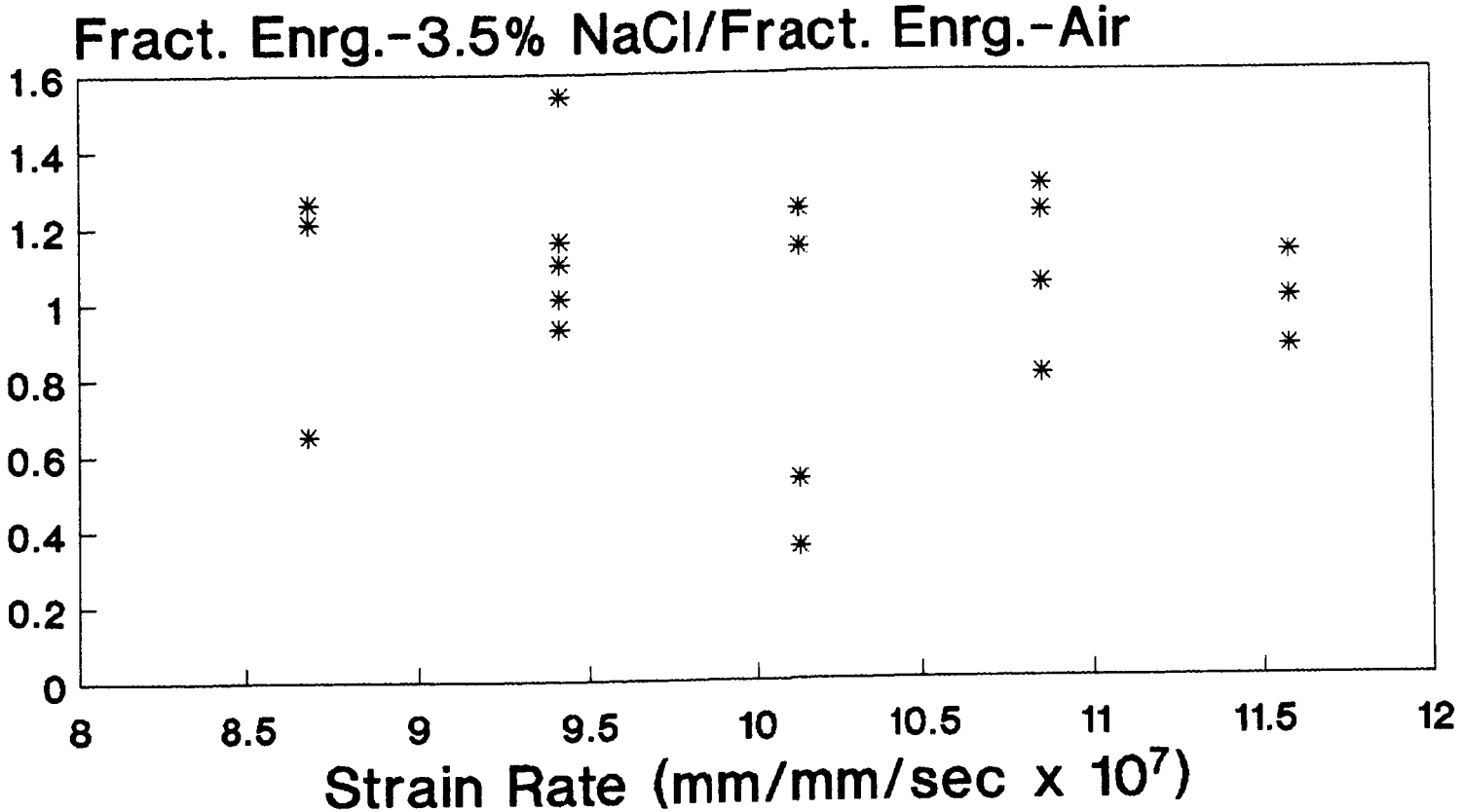

Figure 14. Fracture energy ratio versus strain rate PH13-8Mo H1000.

TECHNICAL REPORT STANDARD TITLE PAGE

1. REPORT NO.	2. GOVERNMENT ACCESSION NO.	3. RECIPIENT'S CATALOG NO.
NASA TP-2934		

4. TITLE AND SUBTITLE	5. REPORT DATE
Stress Corrosion Study of PH13-8Mo Stainless Steel Using the Slow Strain Rate Technique	July 1989
	6. PERFORMING ORGANIZATION CODE
7. AUTHOR(S)	8. PERFORMING ORGANIZATION REPORT #
Pablo D. Torres	
9. PERFORMING ORGANIZATION NAME AND ADDRESS	10. WORK UNIT NO.
George C. Marshall Space Flight Center Marshall Space Flight Center, Alabama 35812	M-613
	11. CONTRACT OR GRANT NO.
	13. TYPE OF REPORT & PERIOD COVERED
12. SPONSORING AGENCY NAME AND ADDRESS	Technical Paper
National Aeronautics and Space Administration Washington, D.C. 20546	14. SPONSORING AGENCY CODE

15. SUPPLEMENTARY NOTES

Prepared by Materials and Processes Laboratory, Science and Engineering Directorate.

16. ABSTRACT

The need for a fast and reliable method to study stress corrosion in metals has caused increased interest in the Slow Strain Rate Technique (SSRT) during the last few decades. In this work, PH13-8Mo H950 and H1000 round tensile specimens were studied by this method. Percent reduction-in-area, time-to-failure, elongation at fracture, and fracture energy were used to express the loss in ductility, which has been used to indicate susceptibility to stress corrosion cracking (SCC). Results from a 3.5 percent salt solution (corrosive medium) were compared to those in air (inert medium). A tendency to early failure was found when testing in the vicinity of 1.0×10^{-6} mm/mm/sec in the 3.5 percent salt solution. PH13-8Mo H1000 was found to be less likely to suffer SCC than PH13-8Mo H950. This program showed that the SSRT is promising for the SCC characterization of metals and results can be obtained in much shorter times (18 hr for PH steels) than those required using conventional techniques.

17. KEY WORDS	18. DISTRIBUTION STATEMENT
Stress Corrosion Slow Strain Rate PH13-8Mo Stainless Steel	Unclassified - Unlimited Subject Category 26

19. SECURITY CLASSIF. (of this report)	20. SECURITY CLASSIF. (of this page)	21. NO. OF PAGES	22. PRICE
Unclassified	Unclassified	32	A03

MSFC - Form 3292 (Rev. December 1972)

For sale by National Technical Information Service, Springfield, Virginia 22161

NASA-Langley, 1989